

ANL-HEP-PR-96-60

November 22, 1996

Isolated Photons at Hadron Colliders at $O(\alpha\alpha_s^2)$ (I): Spin Averaged Case

L. E. Gordon

High Energy Physics Division, Argonne National Laboratory, Argonne, IL 60439

Abstract

The cross sections for isolated and non-isolated prompt photon production with unpolarized hadron beams are studied at order $\alpha\alpha_s^2$. Two methods of performing the calculations are compared. One uses purely analytic techniques and the second uses a combination of analytic and Monte Carlo techniques to perform the phase-space integrations. The results of the analytic and Monte Carlo methods are compared both before and after isolation cuts are placed on the photon. Fragmentation contributions are included at next-to-leading order in the analytic case, and the question of the infrared sensitivity of this contribution once isolation is implemented is addressed. Numerical results are presented and compared with the latest CDF data for $p\bar{p} \rightarrow \gamma + X$ using the latest parton densities for the proton.

Typeset using REVTEX

I. INTRODUCTION

Prompt photon production is now firmly established as one of the most powerful tools for uncovering information on the structure of hadrons and is therefore one of the best ways known for testing perturbative quantum chromodynamics (QCD) [1]. This is due in large part to the fact that photons couple directly to quarks via the well understood point-like electromagnetic interaction, and therefore provide an incisive probe of the short distance dynamics of the hard scattering process involving the strong interaction. Since the cross section for prompt photon production is dominated by the subprocess $qg \rightarrow \gamma q$ in hadronic collisions already in leading order (LO), it has proved very useful for providing information on the gluon distributions, $g(x, Q^2)$, of hadrons at fixed target facilities. At colliders the situation is more complicated due to the necessity of imposing isolation restrictions on the photon in order to identify the signal from among the copious hadronic debris. This restricts the usefulness of the process for extracting information on gluon distributions since isolation is not yet fully understood theoretically and there is some controversy pertaining to the use of the conventional factorization theorem in the infrared regions of phase space for the fragmentation contribution in NLO [2,3] when isolation cuts are imposed. These difficulties are very unwelcome since prompt photon production probes the parton densities of the proton in the region $x \sim x_T = 2p_T^\gamma/\sqrt{s} = 10^{-2}$ for $p_T^\gamma = 10$ GeV at pseudo-rapidity, $\eta = 0$ at the Fermilab TEVATRON. Information gained about the gluon densities at colliders could thus be very important for filling in the gaps left by deep inelastic processes which do not constrain it very tightly.

Unfortunately the comparisons of the theoretical predictions and the collider data have proven to be very problematic. For example, the original comparisons between theoretical predictions and the data from the CDF collaboration [4] showed differences as large as a factor of 1.5 or 2 in the low p_T^γ region, the data always being larger. Since that time things have improved, mainly due to improvements in our knowledge of the parton densities, but significant differences still remained which were made even more problematic by uncertainties

in the theoretical calculations. Despite this, significant progress has also been made on the theoretical front as will be demonstrated in this paper.

Not taking into account calculations done in LO, there have been three previous independent calculations of the isolated prompt photon cross section in NLO. The first attempt was made by Aurenche et al. [5]. In this calculation isolation was implemented approximately from a modification of the inclusive cross section calculated in [6], which was one of the earliest complete NLO calculation ever performed in perturbative QCD. Photon isolation was achieved by modifying the large logarithms which occur in the higher order contributions to the non-fragmentation processes when the photon is produced collinearly to a quark. The fragmentation contributions were calculated in LO and a cut was placed on the remnants of the fragmenting parton, and the fragmentation scale was also modified accordingly. This method, although approximate, retained the most important terms for the isolation procedure, such as logarithms of the half-angle of the isolation cone $\ln \delta$ and thus gave quite accurate results for the isolated cross section. Terms such as $\ln \epsilon$, where ϵ is the energy resolution parameter (introduced in section II) were not all retained, hence the procedure would not give accurate results for very small values of this parameter, but in general, dependence of the cross section on this parameter is not very large. Thus the only major area where the calculation was deficient was in the use of LO matrix elements for the fragmentation contributions and the use of LO asymptotic fragmentation functions, both of which were all that were available at the time.

The next major development was the calculation of Baer et al. [7] which dealt with isolation exactly in NLO for the non-fragmentation contributions by the use of a combination of Monte Carlo and analytic techniques to do the phase space integrals. This method is outlined in section IIB(3). The only drawback of this calculation was again that the fragmentation contributions were included in LO and LO asymptotic fragmentation functions were used.

Important theoretical work was also done by Berger and Qiu who studied the isolated cross section in NLO [8] in some detail. They studied the dependence of the cross section

on the isolation parameters and pointed out that the direct contribution should have a $\ln \epsilon$ dependence by examining the general structure of the isolated cross section in the soft limit. They suggested that the isolated cross section may be conveniently written as the inclusive cross section minus a subtraction piece which removes hadronic energy from around the photon whenever this energy is too large to pass the experimental cuts. Their work helped to clarify many of the theoretical issues and highlighted some of the problems involved in defining the isolated cross section. Their numerical results were based on the two previous calculations of refs. [5,7].

The next independent calculation came with the calculation of Gordon and Vogelsang [9] which was confronted with the CDF data in a paper by Glück et al. [10]. In this paper the isolated cross section was calculated using an approximate isolation method which was developed in [9] from a modification of the inclusive cross sections calculated in [11] for the direct part and in [12] for the fragmentation part. In [9] the basic idea of writing the isolated cross section as the inclusive cross section minus a subtraction piece, suggested by Berger and Qiu [8] was implemented and worked out in detail at the partonic level for both the direct and fragmentation contributions. The most significant improvements made were thus inclusion of the fragmentation contributions in NLO and the use of parton to photon fragmentation functions evolved in NLO QCD [13]. The isolation method used, although, strictly speaking, should be valid only in the limit of a very small isolation cone, just as was the case for that of Aurenche et al., [5], was shown to reproduce many of the features of the exact calculation [9] as well as to improve the agreement between theory and experiment when applied at the Fermilab TEVATRON with the inclusion of fragmentation contributions at NLO [10]. One significant difference between the calculations of Glück et al. [9,10] and Aurenche et al. [5] was that terms such $\ln \epsilon$ were retained in the former, leading to a better behaviour when ϵ is varied.

In [9] we tested the accuracy of our analytical isolation method for various values of the isolation parameters by comparing results to our own version of a Monte Carlo method. In that case the Monte Carlo calculation was obtained from the fully analytic results by

subtracting a piece from the latter that involved the isolation cuts. The subtraction piece was integrated over the restricted phase-space inside the isolation cone by Monte Carlo integration (I refer to [9] for the exact details, but provide an outline in the next section). Our Monte Carlo calculation was thus not entirely independent of our analytic one. The usual combined analytic/Monte Carlo method used in [7] is different as outlined below, and is in many ways more versatile but should in the end give the same results.

Since our results for the isolated cross section were first published there have been attempts, mainly by experimentalists, to compare our results with that of Baer et al. [7] to see if the predictions for the isolated cross section differential in p_T^γ are indeed steeper in the low p_T^γ region after inclusion of the NLO fragmentation contributions, thereby accounting for some of the discrepancy in slope between theoretical predictions and experimental data in this region [14]. Our analysis [9,10] showed clearly that, as one would expect, inclusion of the fragmentation contributions in NLO does indeed give a steeper cross section in this region. Surprisingly a comparison of our numerical results with that from the program of Baer et al. [7] showed that we only had a constant $O(13\%)$ enhancement at *all* p_T^γ values [15]. This result was very puzzling as no one can dispute that the NLO fragmentation contributions do have a steeper p_T^γ dependence than the corresponding LO ones as demonstrated in [10]. The source of this result was thus far not determined as our calculation methods were different and the only thing common in both cases is that both results were compared to the analytic calculation of Aurenche et al. in the non-isolated case [5], and agreement was found. In our case a detailed term-by-term algebraic comparison was also made.

In principle the analytic/Monte Carlo method of Baer et al. should give exactly the same results for the direct contributions to the inclusive prompt photon cross section, before isolation cuts are implemented, as the calculations of Aurenche et al. [5] and Gordon and Vogelsang [11] to within the errors of the Monte Carlo integration if the same parameters are used in the calculations. Once isolation cuts are implemented one may possibly expect the exact Monte Carlo method to give the more accurate results, but since the approximate methods of refs. [6] and [9] retained the most important terms then any differences should

be very small. The results of the calculations of Aurenche et al. refs. [5] and Gordon and Vogelsang [11] agreed for the non-isolated case, and thus any discrepancy between the results of the the calculations of Baer et al. [7] and the isolated cross section [9,10] provides a strong motivation for repeating the calculation of the former and making a more detailed comparison. The main motivation for repeating the Monte Carlo calculation was thus to confirm our conclusions in [9] and [10] and hopefully clear up some of the confusion by finding the source of the discrepancy between our results and that of Baer et al. [7]. Details of the Monte Carlo calculation are repeated in ref. [16] where the polarized cross section is also calculated using the same method. A new feature in the present calculation as compared to Baer et al. [7] is that the various subprocess contributions are kept separate which allows one to tell how much of the cross section is due to qg or $q\bar{q}$ scattering, for example as well as allowing a process by process comparison with the analytic calculation where they were kept separate [11]. This information could be useful if one is interested in the sensitivity of the cross section to the gluon densities. For the polarized case, the present calculation is the first using the analytic/Monte Carlo method.

In this paper I therefore compare again the analytic results with the Monte Carlo results, where in this case, Monte Carlo means the full independent analytic/Monte Carlo method. It will be shown that the two methods agree extremely well both before and after isolation cuts are implemented. It turns out that the discrepancy between the results of Baer et al. [7] and Glück et al. [10] was due to an error in the version of the code of the former used by the experimentalists. This error caused the non-fragmentation part of the predicted cross section to have a steeper p_T^γ dependence than those of both Aurenche et al. [6] and [9,10] even before isolation cuts are imposed. It also had the unfortunate effect of cancelling out the increase in slope due to the inclusion of the NLO fragmentation contributions after isolation, given the choice of cut-off parameters used. Another choice of cut-off parameters would likely have given very different results.

All calculations now agree fully for the direct contribution, and it is therefore now possible to study whether the use of modern parton distributions coupled with the inclusion

of the NLO fragmentation contributions will improve the agreement between theory and experiment. This will have a direct bearing on recent studies [17] which suggested that initial state gluon radiation can be used to explain the difference in slope between theory and data. A reduction of the discrepancy would suggest that less initial state radiation would be needed.

The rest of this paper is as follows; In section II a brief theoretical background to the calculations is given including an outline of the analytic/Monte Carlo method used, as well as the approximate analytic method of isolation. In section III a fairly detailed comparison of the analytic and Monte Carlo methods is made and comparisons with the CDF data is presented, and in section IV the conclusions are given.

II. ISOLATED PROMPT PHOTONS

In this section I briefly outline the calculational techniques used to obtain the inclusive and isolated prompt photon cross sections in both the analytic and Monte Carlo cases.

Contributions to the prompt photon cross section are usually separated into two classes in both LO and NLO. There are the so-called direct processes, $ab \rightarrow \gamma c$ in LO and $ab \rightarrow \gamma cd$, in NLO, a, b, c and d referring to partons, where the photon is produced directly in the hard scattering. In addition there are the fragmentation contributions where the photon is produced via bremsstrahlung off a final state quark or gluon, $ab \rightarrow cd(e)$ followed by $c \rightarrow \gamma + X$ for instance.

Experimentally, a prompt photon is considered isolated if inside a cone of radius R centered on the photon the hadronic energy is less than ϵE_γ , where E_γ is the photon energy and ϵ is the energy resolution parameter, typically $\epsilon \sim 0.1$. The radius of the circle defined by the isolation cone is given in the pseudo-rapidity η and azimuthal angle ϕ -plane by $R = \sqrt{(\Delta\eta)^2 + (\Delta\phi)^2}$. In the case of a small cone the parameter used is the half angle of the cone, δ , where $\delta \approx R$ for small rapidities of the photon. The exact relation is $R = \delta/\cosh\eta$.

A. The LO Case

In LO, $O(\alpha\alpha_s)$, the direct subprocesses contributing to the cross section are

$$\begin{aligned} qg &\rightarrow \gamma q \\ q\bar{q} &\rightarrow \gamma g. \end{aligned} \tag{2.1}$$

In addition there are the fragmentation processes

$$\begin{aligned} qg &\rightarrow qg \\ qq &\rightarrow qq \\ qq' &\rightarrow qq' \\ q\bar{q} &\rightarrow q\bar{q} \\ qg &\rightarrow qg \\ q\bar{q} &\rightarrow gg \\ gg &\rightarrow gg \\ gg &\rightarrow q\bar{q} \end{aligned} \tag{2.2}$$

where one of the final state partons fragments to produce the photon, i.e., $q(g) \rightarrow \gamma + X$.

In the direct processes in LO, the photon is always isolated since it must always balance the transverse momentum p_T of the other final state parton and is thus always in the opposite hemisphere. In this case the differential cross section is given by

$$E_\gamma \frac{d\sigma_{dir}^{LO}}{d^3p_\gamma} = \frac{1}{\pi S} \sum_{i,j} \int_{VW}^V \frac{dv}{1-v} \int_{VW/v}^1 f_1^a(x_1, M^2) f_2^b(x_2, M^2) \frac{1}{v} \frac{d\hat{\sigma}_{ab \rightarrow \gamma}}{dv} \delta(1-w) \tag{2.3}$$

where $S = (P_1 + P_2)^2$, $V = 1 + T/S$, $W = -U/(T + S)$, $v = 1 + \hat{t}/\hat{s}$, $w = -\hat{u}/(\hat{t} + \hat{s})$, $\hat{s} = x_1 x_2 S$, and $T = (P_1 - P_\gamma)^2$ and $U = (P_2 - P_\gamma)^2$. As usual the Mandelstam variables are defined in the upper case for the hadron-hadron system and in lower case in the parton-parton system. P_1 and P_2 are the momenta of the incoming hadrons and $f_1^a(x_1, M^2)$ and $f_2^b(x_2, M^2)$ represent the respective probabilities of finding parton i and j in hadrons 1 and 2 with momentum fractions x_1 and x_2 at scale M^2 .

For the fragmentation processes, the photon is always produced nearly collinearly to the fragmenting parton and an isolation cut must be placed on the cross section to remove the remnants of the fragmenting parton if it has more energy than ϵE_γ . In this case this restriction is quite easy to implement. The inclusive differential cross section is given by

$$E_\gamma \frac{d\sigma_{frag}^{incl}}{d^3 p_\gamma} = \frac{1}{\pi S} \sum_{a,b,c} \int_{1-V+VW}^1 \frac{dz}{z^2} \int_{VW/z}^{1-(1-V)/z} \frac{dv}{1-v} \int_{VW/vz}^1 \frac{dw}{w} f_1^a(x_1, M^2) f_2^b(x_2, M^2) \times \frac{1}{v} \frac{d\hat{\sigma}_{ab \rightarrow c}}{dv} \delta(1-w) D_c^\gamma(z, M_f^2), \quad (2.4)$$

where $D_{\gamma/c}(z, M_f^2)$ represents the probability that the parton labelled c fragments to a photon with a momentum fraction z of its own momentum at scale M_f^2 . This is the non-perturbative fragmentation function which must be obtained from experiment at some scale and evolved to M_f^2 using the usual evolution equations. This means that in order to obtain the isolated cross section we simply have to cut on the variable z . If isolation is defined in the usual way by only accepting events with hadronic energy less than fraction ϵ in a cone of radius $R = \sqrt{(\Delta\phi)^2 + (\Delta\eta)^2}$ drawn in the pseudo-rapidity azimuthal angle plane around the photon, then the hadronic remnants of the fragmenting parton will always automatically be inside the cone with the photon, for suitable choices of M_f , and the isolated cross section is given by the equation

$$E_\gamma \frac{d\sigma_{frag}^{isol}}{d^3 p_\gamma} = \frac{1}{\pi S} \sum_{a,b,c} \int_{MAX[z_{min}, 1/(1+\epsilon)]}^1 \frac{dz}{z^2} \int_{VW/z}^{1-(1-V)/z} \frac{dv}{1-v} \int_{VW/vz}^1 \frac{dw}{w} f_1^a(x_1, M^2) f_2^b(x_2, M^2) \times \frac{1}{v} \frac{d\hat{\sigma}_{ab \rightarrow c}}{dv} \delta(1-w) D_c^\gamma(z, M_f^2), \quad (2.5)$$

where $z_{min} = 1-V+VW$. It is also suggested that the fragmentation scale should be replaced by (RM_f) or (δM_f) in order to ensure that all fragmentation remnants are radiated inside the cone [8], but this argument not universally accepted. It was shown in [9] that the choice is numerically irrelevant, since the dependence of the cross section on the fragmentation scale is negligible after isolation in NLO.

B. The NLO Case

1. The Non-Fragmentation Contribution

At $O(\alpha\alpha_s^2)$ there are virtual corrections to the LO non-fragmentation processes of eq.(2.1), as well as the further three-body processes:

$$g + q \rightarrow g + q + \gamma \quad (2.6a)$$

$$g + g \rightarrow q + \bar{q} + \gamma \quad (2.6b)$$

$$q + \bar{q} \rightarrow g + g + \gamma \quad (2.6c)$$

$$q + q \rightarrow q + q + \gamma \quad (2.6d)$$

$$\bar{q} + q \rightarrow \bar{q} + q + \gamma \quad (2.6e)$$

$$q + \bar{q} \rightarrow q' + \bar{q}' + \gamma \quad (2.6f)$$

$$q + q' \rightarrow q + q' + \gamma \quad (2.6g)$$

In principle the fragmentation processes of eq.(2.2) should now be calculated to $O(\alpha_s^3)$ and convoluted with the NLO photon fragmentation functions whose leading behaviour is $O(\alpha/\alpha_s)$ leading to contributions of $O(\alpha\alpha_s^2)$. For the inclusive cross section fragmentation processes can contribute 50–60% of the cross section at the lowest p_T^γ values at TEVATRON energies. Numerically the fragmentation processes are not as significant after isolation cuts are implemented, but for a theoretically consistent calculation they should nevertheless be included as they help to reduce scale dependences, and as was demonstrated in ref. [10] they also help to improve the agreement between theory and experiment in the low p_T^γ region.

The direct contribution to the inclusive cross section is given by

$$E_\gamma \frac{d\sigma_{dir}^{incl}}{d^3p_\gamma} = \frac{1}{\pi S} \sum_{a,b} \int_{VW}^V \frac{dv}{1-v} \int_{VW/v}^1 \frac{dw}{w} f_1^a(x_1, M^2) f_2^b(x_2, M^2) \times \left[\frac{1}{v} \frac{d\hat{\sigma}_{ab \rightarrow \gamma}}{dv} \delta(1-w) + \frac{\alpha_s(\mu^2)}{2\pi} K_{ab \rightarrow \gamma}(\hat{s}, v, w, \mu^2, M^2, M_f^2) \right], \quad (2.7)$$

where $K_{ab \rightarrow \gamma}(\hat{s}, v, w, \mu^2, M^2, M_f^2)$ represents the higher corrections to the hard subprocess cross sections calculated in [11] and μ is the renormalization scale.

In [9] the isolated cross section is written as the inclusive cross section minus a subtraction piece as first suggested in [8]

$$E_\gamma \frac{d\sigma_{dir}^{isol}}{d^3 p_\gamma} = E_\gamma \frac{d\sigma_{dir}^{incl}}{d^3 p_\gamma} - E_\gamma \frac{d\sigma_{dir}^{sub}}{d^3 p_\gamma}, \quad (2.8)$$

$E_\gamma \frac{d\sigma_{dir}^{sub}}{d^3 p_\gamma}$ being the cross section for producing a prompt photon with energy E_γ which is accompanied by more hadronic energy than ϵE_γ inside the cone. The question is then how to calculate the subtraction piece. In [9] it is calculated by an approximate analytic method for a small cone of half angle δ as well as for a cone of radius R as defined above using Monte Carlo integration methods. The complete details of the calculation can be found in ref. [9]. The final form for the subtraction piece assuming a small cone of half angle δ is given by

$$E_\gamma \frac{d^3 \sigma_{dir}^{sub}}{d^3 p_\gamma} = A \ln \delta + B + C \delta^2 \ln \epsilon, \quad (2.9)$$

where A , B and C are functions of the kinematic variables of the photon and ϵ . The functions A , B and C were calculated in ref. [9] and can be found in the appendix of that paper. As noted earlier there is a term proportional $\ln \epsilon$ as anticipated in ref. [8] which was not retained in ref. [5]. A detailed study was then made of the difference between the analytic and numerical Monte Carlo *subtraction* pieces for various values of the isolation parameters ϵ and δ at $\sqrt{S} = 1$ TeV for the direct contribution. It was found that the small cone approximation was within 10% of the Monte Carlo results for the subtraction piece except for very large values of ϵ and δ , greater than 0.25 and 0.8 respectively. This translated into a *very small* error for the *full* isolated cross section even for large values of the parameters, as the subtraction piece is numerically much smaller than the inclusive piece. For example, at $p_T^\gamma = 15$ GeV the subtraction piece is less than 10% of the direct contribution to the isolated cross section.

2. The Fragmentation Contribution

A similar method was employed for the fragmentation contribution in NLO and although a comparison with a Monte Carlo calculated version could not be made, it was quite reasonably assumed that the result from the direct study could be carried over, at least as far as numerical accuracy is concerned. In this case the analytic method consists of imposing

a cut on the remnants of the fragmenting parton, just as in the LO case, by imposing the restriction $z \geq \text{MAX}[z_{min}, 1/(1+\epsilon)]$ on the integration over z . In NLO this cut is no longer sufficient to isolate the photon, since there is now a third parton in the final state which may also be radiated into the isolation cone. In ref. [9] this is dealt with by calculating a subtraction piece, similar to the direct case which removes the contribution to the cross section whenever this third parton is in the cone, and is radiated collinearly to the fragmenting parton, providing that the sum of its energy plus the energy of the remnants of the fragmenting parton is above the threshold, ϵE_γ . Thus the fragmentation contribution to the isolated cross section is

$$E_\gamma \frac{d\sigma_{frag}^{isol}}{d^3 p_\gamma} = E_\gamma \frac{d\sigma_{frag}^{z \geq \frac{1}{1+\epsilon}}}{d^3 p_\gamma} - E_\gamma \frac{d\sigma_{frag}^{sub}}{d^3 p_\gamma}, \quad (2.10)$$

where the first term on the RHS is the NLO cross section with the insufficient z -cut implemented and the second term is the cross section with the additional parton in the cone. Schematically the subtraction piece is given approximately by

$$E_\gamma \frac{d^3 \sigma_{frag}^{sub}}{d^3 p_\gamma} = \epsilon^a \left[\ln \delta (A + A' \ln \delta) + B + C \delta^2 \ln \epsilon \right], \quad (2.11)$$

with new coefficients A, A', B and C , all of which were calculated in [9].

In [9] it was not practical to test the accuracy of the analytic method for isolating fragmentation contribution because of the complexity of the NLO matrix elements. Its accuracy was therefore assumed to be similar to the direct piece. This assumption is resonable, but it would nevertheless be desirable to test it. Work is currently underway to test the accuracy of the method by considering the less complex photoproduction processes $\gamma q \rightarrow qgg$ and $\gamma g \rightarrow q\bar{q}g$. The final states of these processes are the same as those of $gq \rightarrow qgg$ and $gg \rightarrow q\bar{q}g$ which are two of the processes found for the hadron-hadron case. Any conclusion drawn about the accuracy of the isolation method from these processes can be generalized to the hadron-hadron case. For the purposes of the present work however, it is assumed that the method is as accurate for fragmentation as it is for the direct piece.

Before leaving this section it should be noted that according to ref. [2] there is a serious problem with the definition of the isolated cross section in the fragmentation case. They

concluded that conventional factorization breaks down in the fragmentation case when isolation restrictions are imposed on the photon. Thus the cross section can no longer be written in the schematic factorized form

$$\sigma = f_a(x_a, M^2) * f_b(x_b, M^2) * \hat{\sigma}^{ab \rightarrow cX} * D_c^\gamma(z, M_f^2), \quad (2.12)$$

where the hard scattering cross section, $\hat{\sigma}^{ab \rightarrow cX}$ is infrared finite. They calculated the cross section for the process $e^+e^- \rightarrow \gamma + X$ and found it not to be infrared finite when the photon is isolated.

Arguments were also presented in ref. [2] for the hadron-hadron case with the conclusion that it has an integrable logarithmic divergence which renders the calculation unreliable. The cross section differentiable in a specific variable for the subprocess $q\bar{q} \rightarrow q'\bar{q}'g$ with subsequent fragmentation of one of the final state quarks was studied and found to be larger than the corresponding inclusive cross section in the region of phase space where a soft gluon is radiated into the isolation cone. This situation would be unphysical since the phase space for the isolated cross section is more restricted than for the non-isolated case. These conclusions were disputed in ref. [3] where arguments were given to support the view that the physical cross section is singularity free and thus well defined. While it is not the purpose of this paper to support either position for the general case, I shall nevertheless show that the calculation presented here for the fragmentation contribution in NLO as calculated in [9] is well defined and regular in all regions of phase space. In fact the large logarithms mentioned in ref. [2] are well behaved and regulated in the limit where the gluon becomes soft as they should be for any well defined cross section, and therefore cannot render the isolated cross section unreliable.

My argument will rest on the following three points;

1. Integration over the kinematic variables w and z is necessary in order to define the physical cross section whether the photon is isolated or not.
2. Only the subtraction piece of the cross section defined in equation (2.10), namely

$E_\gamma d\sigma_{sub}^{frag} / d^3 p_\gamma$, can potentially have any soft divergence associated with the isolation procedure.

3. All potential soft divergences are well regulated in the physically measurable cross section.

Let us address point (1) by first noting that in this calculation the soft gluon limit is the limit $w \rightarrow 1$ for *both* terms on the RHS of eq.(2.10), thus the soft gluon limit is a clearly identifiable and unique point in the calculation as it should be since the two parts are not independent but together make up the isolated cross section. One can thus compare how the soft limit is approached for each part and make sure that this point is neither over counted or under counted in the definition of the isolated cross section. If the point is counted twice then clearly extra soft singularities would be created and the cross section would not be finite. If the point is not counted at all then this would lead to uncanceled soft singularities in the virtual piece with the same result.

In the case of the first term of the right of eq.(2.10) the soft divergences are regulated by ‘plus’-distributions such as $1/(1-w)_+$ which are defined to be regular in the soft limit for integration of a test function $f(w)$, not singular at $w = 1$, over w by the equation

$$\int_A^1 \frac{f(w)}{(1-w)_+} dw = \int_A^1 \frac{f(w) - f(1)}{1-w} dw + \ln(1-A)f(1). \quad (2.13)$$

Thus the first term of eq.(2.10) is only defined and regular if an integration over w is performed over a finite region when w is near 1. Note also that although the divergences are regulated, near this point the region of integration cannot be taken too narrow because even without isolation the cross section would become infrared sensitive, i.e. if A is too near to 1 then $\ln(1-A)$ would diverge. This type of infrared sensitivity is well known in perturbative QCD and can only be cured by soft gluon resummation. The lower limit of integration over w , A , is set by external kinematics in the hadronic system and is not affected by the isolation cuts. Clearly then the isolated cross section of eq.(2.10) is only defined when integration over w is performed.

Point (2) is easily shown to be true. The first term on the right of eq.(2.10), $E_\gamma d\sigma_{frag}^{z \geq \frac{1}{1+\epsilon}} / d^3 p_\gamma$, involves a cut on the variable z only and this occurs after the soft limit $w \rightarrow 1$ is regulated by the procedure defined by eq.(2.13). In other words, placing a cut on the remnants of the fragmenting quark alone does not place any restrictions on the phase space available to the gluon. This means no divergent logarithms associated with the isolation procedure can come from this term.

Point (3) is the most important and must be examined carefully. To see where a divergence may potentially occur in our treatment of the isolated cross section we must examine the structure of the subtraction piece. If we assume that a fragmenting quark with original energy E_q and final energy E'_q plus a gluon with energy E_g are inside the cone, then the isolation condition is

$$E_g + E'_q > \epsilon E_\gamma \quad (2.14)$$

for the subtraction piece. This translates to a condition

$$z(1 + \epsilon) < \frac{1}{1 - v + vw} \quad (2.15)$$

on the phase space for the subtraction piece. In ref. [9], in the small cone limit, the subtraction cross section was written as

$$E_\gamma \frac{d\sigma_{frag}^{sub}}{d^3 p_\gamma} = \frac{1}{\pi p_T^2 S} \sum_{abc} \int_{\max(1-V+VW, \frac{1}{1+\epsilon})}^1 dz \int_{VW/z}^{1-(1-V)/z} dv \int_{VW/zv}^1 dw \times f_1^a(x_1, M^2) f_2^b(x_2, M^2) D_c^\gamma(z, M_f^2) \hat{s} \frac{d\hat{\sigma}_\delta^{ab \rightarrow c}}{dv dw} \Theta\left(\frac{1}{1 - v + vw} - z(1 + \epsilon)\right), \quad (2.16)$$

where the kinematic variables are defined as before, and $d\hat{\sigma}_\delta^{ab \rightarrow c} / dv dw$ is the hard cross section in the small cone approximation. Consider, for example, the process $qg \rightarrow qX \rightarrow \gamma X'$ where the photon is produced by fragmentation off a quark. In the small cone/collinear limit the hard cross section is given by

$$\frac{d\hat{\sigma}_\delta^{qg \rightarrow q}}{dv dw} = \frac{\alpha_s}{2\pi} \frac{v}{1 - v + vw} \times \left[P_{qg}(1 - v + vw) \frac{d\hat{\sigma}^{qg \rightarrow qg}(\hat{s}, y)}{dy} + P_{gg}(1 - v + vw) \frac{d\hat{\sigma}^{qg \rightarrow gg}(\hat{s}, y)}{dy} \right], \quad (2.17)$$

where $y = vw/(1 - v + vw)$, and the splitting functions are given by

$$\begin{aligned} P_{qq}(z) &= C_F \left[\frac{1+z^2}{1-z} \ln \left(\frac{v^2(1-w)^2 E_\gamma^2 \delta^2}{z^2 M_f^2} \right) + (1-z) \right] \\ P_{qg}(z) &= \left[\frac{z^2 + (1-z)^2}{z} \ln \left(\frac{v^2(1-w)^2 E_\gamma^2 \delta^2}{z^2 M_f^2} \right) + z(1-z) \right]. \end{aligned} \quad (2.18)$$

The splitting function $P_{qq}(z)$ where $z = 1 - v + vw$ has a $1/(1-w)$ behavior which, after integration over w behaves as $\ln(1-w)$. In eq.(2.16), the upper limit of the w integration is

$$1 - \frac{1}{v} + \frac{1}{zv(1+\epsilon)},$$

which is 1 if $z = 1/(1+\epsilon)$. This occurs when the energy of the gluon inside the cone, $E_g = 0$ and therefore $E'_q = \epsilon E_\gamma$, i.e., at the lower limit of the z integration in eq.(2.16), the logarithm $\ln[(1-(1+\epsilon)z)/((1+\epsilon) vz)]$ becomes $\ln[0]$. This apparent logarithmic divergence, if not regulated, could render the subtraction piece, and therefore the full fragmentation contribution to the isolated cross section unreliable. We must therefore examine how the subtraction piece actually behaves in this limit.

From a physical point of view we do not want to subtract the contribution to the cross section when $E_g = 0$ inside the cone as this passes the isolation cut and hence is part of the measured cross section. This point is included in the first term on the RHS of eq.(2.10) where the poles have been cancelled in $4 - 2\epsilon$ dimensions and all attendant divergences have been regulated by the ‘plus’-distributions. Thus when this limit is approached in the subtraction piece, the subtraction piece should give no contribution and should ideally vanish. In an approximate calculation the subtraction piece may still give a (small) finite contribution in this limit, but there should be no divergent logarithms present. This is the justification for doing the rest of the phase space integrals in 4-dimensions. We thus need to ensure that there are no divergent logarithms in the soft limit of the subtraction piece that would render the predictions unreliable. In fact the potential singularity is actually regulated and is therefore *not* dangerous as long as we integrate over the variables w and z , as required for the definition of the physical cross section.

From eqs.(2.17) and (2.18) the term proportional to $1/(1 - w)$ would be the first potentially dangerous term. Let us for the moment ignore the dependence of the structure and fragmentation functions on the variables z and w . In fact the fragmentation function is actually small at the point $z = 1/(1 + \epsilon)$ which is near to $z = 1$ where it vanishes. It turns out that when we integrate over w and z this singular term becomes

$$\left[\left(\frac{1}{1 + \epsilon} - z \right) \ln[z(1 + \epsilon) - 1] + z \ln[z(1 + \epsilon)] \right]_{\frac{1}{1 + \epsilon}}^1 \quad (2.19)$$

which clearly vanishes in the limit $z \rightarrow 1/(1 + \epsilon)$ as it should. A similar situation occurs for the term $\ln(1 - w)/(1 - w)$. The conclusion is thus that there are no unregulated soft divergences in the cross section defined by eq.(2.16), and thus also not in that of eq.(2.10). This behaviour is supported by the results of the numerical calculation where the integral converges smoothly to a finite limit.

One may argue that if the integrand as a function of w is singular when $w \rightarrow 1$ then the predictions could be unreliable. If one were to plot a curve of $d\hat{\sigma}/dvdw$, the hard subprocess cross section, versus w , whenever $w = 1$ a singularity would be encountered. Of course this singular point would also be encountered for the fully inclusive subprocess cross section. As stated above the hard subprocess cross section in both the inclusive and isolated cases are defined in terms of ‘plus’-distributions such as $1/(1 - w)_+$ and $[\ln(1 - w)/(1 - w)]_+$ which have no meaning at $w = 1$ unless one integrates over a finite region including this point to define a physically observable cross section. Thus plotting the hard subprocess cross sections vs w is meaningless as no conclusions could be drawn from the result.

The conclusion is therefore that although it is generally accepted that further work is needed in order to fully deal with isolation in the fragmentation case at both leading and next to leading order, mostly to do with defining the fragmentation functions when the isolation restrictions are imposed, for the well defined physical cross section presented here there are no soft divergences which survive to make the predictions unreliable.

3. The Monte Carlo Method

The Monte Carlo method was first used in [7] for the unpolarized case and a detailed description can be found there so only an outline is presented here. Some details are also presented in ref. [16] where the polarized case is highlighted. When the two-to-three hard scattering subprocesses are integrated over phase space, singularities are encountered whenever a gluon becomes soft or two partons become collinear. Some of these singularities will cancel against similar ones in the virtual two-body contributions. The rest are factored into the parton distribution and fragmentation functions at some arbitrary scale, or cancelled when an appropriate jet definition is implemented. The Monte Carlo technique consists essentially in identifying those regions of phase space where soft and collinear singularities occur and integrating over them analytically in $4 - 2\epsilon$ dimensions, thereby exposing the singularities as poles in ϵ . In order to isolate these regions from the rest of the three-body phase space arbitrary boundaries are imposed through the introduction of cutoff parameters, δ_s and δ_c . The soft gluon region of phase space is defined to be the region in which the gluon energy, in a specified reference frame, usually the subprocess rest frame, falls below a certain threshold, $\delta_s\sqrt{\hat{s}}/2$, where δ_s is the cutoff parameter, and \hat{s} is the center-of-mass energy in the initial parton-parton system. Labelling the momenta for the general three-body process by $p_1 + p_2 \rightarrow p_3 + p_4 + p_5$, the general invariants are defined by $s_{ij} = (p_i + p_j)^2$ and $t_{ij} = (p_i - p_j)^2$. The collinear region is defined as the region in which the value of an invariant falls below the value $\delta_c\hat{s}$.

Specific approximate versions of the full three-body matrix elements are integrated over the soft and collinear regions of phase space. For the soft-gluon case the approximate matrix element is obtained by setting the gluon energy to zero everywhere it occurs in the matrix elements, except in the denominators. For the collinear singularities, each invariant that vanishes is in turn set to zero everywhere except in the denominator. This form is the leading pole approximation. These approximate expressions are then integrated over phase space and only the terms proportional to logarithms of the cutoff parameters are retained.

All terms proportional to positive powers of the cutoff parameters are set to zero. Therefore in order for the method to yield reliable results, the cutoff parameters must be kept small, otherwise the approximations would not be valid.

Once the two-to-three particle phase space integrals are performed analytically over the singular regions exposing the soft and collinear poles, the $O(\alpha_s^2)$ virtual gluon-exchange loop contributions, if these are present, are added, and all double and single poles are verified to cancel, as they should. The remaining collinear singularities are factored into parton distribution and fragmentation functions at an appropriate factorization or fragmentation scale, after an appropriate factorization scheme is chosen. In this calculation I use the \overline{MS} scheme. One is now left with a set of matrix elements for effective two-body final-state processes that depend explicitly on $\ln \delta_s$ and $\ln \delta_c$. In addition, the non-singular regions of phase space yield a set of three-body final-state matrix elements which, when integrated over phase space by Monte Carlo techniques, have an implicit dependence on these same logarithms. The signs are such that the dependences on $\ln \delta_s$ and $\ln \delta_c$ cancel between the two-body and three-body contributions. The physical cross sections are independent of these arbitrary cutoff parameters over wide ranges. All the two and three-body matrix elements for both the polarized and unpolarized calculation are presented in the appendix of ref. [16].

The Monte Carlo method outlined above is well suited to calculations of processes involving well defined experimental selections such as isolation cuts. Since all singularities have already been cancelled, whenever an event fails an experimental cut it is simply rejected and does not contribute to the cross section. As emphasized earlier, at colliders it is necessary to restrict the hadronic energy allowed near the photon in order that the signal may be identified unambiguously. In the method of calculation just outlined here the isolation cuts can be implemented exactly.

III. NUMERICAL RESULTS

In this section numerical results are presented for the cross section at a center-of-mass energy of $\sqrt{s} = 1.8$ TeV appropriate for the CDF and D0 experiments at Fermilab. First a comparison is made between the cross sections calculated using purely analytic methods and using the Monte Carlo technique. In these comparisons the fragmentation contributions are included with LO matrix elements only, whereas the direct ones are always calculated in NLO. Later when a comparison with the CDF data is made then the fragmentation contribution calculated using the approximate analytic method at NLO is included. In all cases where LO matrix elements are used, the parton densities and fragmentation functions evolved in NLO are nevertheless used.

The renormalization, factorization, and fragmentation scales are always set to a common value $\mu = p_T^\gamma$ unless otherwise stated. The fragmentation functions evolved in NLO from ref. [13] are used throughout, but various parametrizations of the parton densities of the proton are used. The NLO two-loop expression for α_s is always used and four quark flavors are assumed ($N_f = 4$). The value of Λ used is chosen to correspond with the parton densities in use.

A. Analytic vs Monte Carlo Isolation Methods

The Monte Carlo and analytic methods of calculating the inclusive cross section should give the same results for the same choice of parameters. This can serve as a check on both calculations. In fig.1a the predictions are compared for the standard choice of parton distributions in this subsection, the CTEQ3M set [18] at $\sqrt{s} = 1.8$ TeV. Clearly they agree over many decades of p_T^γ as they should. In fact the numerical differences are generally less than 4% and are always within the errors of the Monte Carlo calculation. For the isolated cross section, the analytic calculation is only strictly valid for a very small cone and small values of the energy resolution parameter ϵ , so it is interesting to see whether it gives

similar predictions to the Monte Carlo for CDF parameters, $R \sim \delta = 0.7$ and $\epsilon = 2\text{GeV}/p_T^\gamma$. Fig.1b compares the isolated cross section as predicted by the analytic and Monte Carlo calculations. From this graph it can be seen they agree extremely well at all p_T^γ values shown. Again at no point is there a difference of more than $\pm 3 - 4\%$ between the two, and the differences are always within the Monte Carlo errors. Fig.1c shows the predictions of the Monte Carlo calculation broken down into some of the subprocess contributions. This graph confirms that the cross section is dominated by initial qg scattering but also shows that $q\bar{q}$ scattering is important especially in the large p_T^γ region.

In figs.2a and 2b the dependences on ϵ and R are compared at two values of p_T^γ . In the case of ϵ dependence the results are very similar except at very small values of ϵ where the analytic results tend to be larger. This feature was noted in ref. [9] where it was shown that the analytic calculation is more accurate at lower p_T^γ . For the R dependence there is a larger discrepancy between the two curves for $R \leq 0.3$. It seems that the analytic calculation gives results which are too large in this region, and for $R \leq 0.1$ gives results which are even larger than the inclusive one. Clearly the analytic approximation is breaking down at this point. This is understandable since only terms such as $\ln \delta$ are retained which give a large negative contribution to the subtraction piece of the cross section. Thus there appears to be a point below which the analytic approximation does not give reliable results, despite the fact that in principle it should be valid for a small cone. For all values of R above 0.4 the two methods give essentially identical results, hence the small cone approximation should be reliable for CDF isolation parameters.

B. Comparison with CDF Data

Now that we have established that the analytic and Monte Carlo methods give essentially the same results for the isolated cross section at CDF we are in a position to compare predictions with data. An interesting question concerning the NLO calculation as presented here is how much of the cross section is due to the fragmentation contribution, and how

much enhancement does the inclusion of the NLO fragmentation contributions bring. To answer this question, in fig.3a the ratio

$$\frac{\sigma^{frag}}{\sigma^{dir} + \sigma^{frag}}$$

is plotted for the isolated cross section with CDF parameters. σ^{dir} is the direct contribution to the cross section in NLO, whereas σ^{frag} is calculated both with LO (dashed line) and with NLO matrix elements (solid line). As one may expect, the fragmentation contributions are most important at low p_T^γ . When it is calculated in NLO the fragmentation contribution clearly gives a larger contribution to the cross section, indicating that a better agreement with the CDF data, which are generally steeper than the theoretical predictions may be expected in this case. To further highlight this point, in fig.3b the ratio

$$\frac{\sigma^{dir} + \sigma^{frag}(NLO)}{\sigma^{dir} + \sigma^{frag}(LO)}$$

is plotted for both the isolated and non-isolated cases. The denominator corresponds to predictions made by the calculation of ref. [7], where the fragmentation contributions are included with LO matrix elements. The NLO fragmentation contributions give up to 15% enhancement to the cross section at low p_T^γ for the isolated case. Comparison with the non-isolated case indicates that the effect of the NLO fragmentation contributions are suppressed relative to the LO ones after isolation cuts are imposed. This is not surprising since isolation involves a more severe restriction on the three-body phase space of the NLO contributions but similar restrictions on the two-body phase space parts of both the LO and NLO calculations.

In fig.4a a comparison is made with the CDF data for the isolated cross section and the full NLO calculation using various parton densities labelled MRSR [19], CTEQ3M [18] and GRV94 [20]. In the case of the GRV94 distributions, no charm contribution was included in the parametrization, the intention being that the contribution due to charm quark scattering be calculated using matrix elements that explicitly take the charm quark mass into account. Since these matrix elements are not yet available in NLO, the GRV94 curve has been supplemented by including a charm density from their older parametrization, [21]. This enhances

the cross section by about 20% in the low p_T^γ region and allows an easier shape comparison with the curves from the other parton densities. From fig.4a it appears that all the curves agree reasonably well with the data, with MRSR4 perhaps giving a better description of the data in the low p_T^γ region. Fig.4b which highlights this problematic region confirms this.

A more detailed comparison with the data is made in fig.4c where the quantity

$$\frac{DATA - THEORY}{THEORY}$$

is plotted. If data and theory agreed exactly then this line would ideally be a straight line through 0. The data is compared directly to the MRSR2 parametrization, and taking this set as the default, the results using the other sets are substituted for the data and also plotted in the figure. A similar procedure is carried out in fig.4d, but there taking the CTEQ4HJ set, which is fitted to the new CDF large p_T jet data [22] as the default. There is a substantial spread in the curves and taken as a whole the band they provide describes the data well. But taken individually they clearly all leave some slope difference with the data taken as a whole. This slope is substantially diminished when compared to most previous comparisons with the data [4], partly due to the enhancement from the fragmentation and partly due to the modern, steeper parton distributions. Even recently there was up to 40% difference between the theoretical curves and the data at low p_T^γ whereas now, for the steepest distributions, this is reduced to under 10%. The overall slope in the data taken over all p_T^γ values for the MRSR2 parametrization is roughly 20%, whereas the systematic uncertainty as reported by CDF is of order 5%.

A change in the factorization/renormalization scales from $\mu^2 = (p_T^\gamma)^2$ to $\mu^2 = (p_T^\gamma/2)^2$ does not affect the slope of the curves substantially in the p_T range considered here. The major effect of this change in the scale is a normalization shift of all the curves upwards. This uncertainty in the theoretical predictions therefore cannot be exploited to explain the slight slope difference between the data and theory. Although the parton distributions are much better known than they were a few years ago, as the differences between the various curves clearly show, there is still enough uncertainty here, particularly in the gluon distributions, to

explain at least some of the slope differences. Another area which has also been explored with some success [15] is inclusion of initial state transverse momentum k_T effects due to soft gluon radiation off the initial state partons. There is also the possibility that estimates of the NLO fragmentation contributions could be improved via either better theoretical treatment of the isolation conditions on the matrix elements or on the fragmentation functions themselves. But although this may have some effect on the predictions at low p_T^γ it will not affect substantially the predictions above $p_T^\gamma = 30 - 40$ GeV, where the theory over predicts the data by an almost constant 10%.

An interesting and rather curious thing to observe about the discrepancy between the theoretical predictions and the data is that if one were to separate the high (≥ 30) GeV and the the low p_T^γ regions then the theoretical predictions could be made to fit the data in these regions separately with different structure functions. For example MRSR4 describes the low p_T^γ data extremely well (fig.5a), whereas MRSR1 does very well at high p_T^γ (fig.5b). Of course if the data is examined between $p_T^\gamma \sim 15$ and 30 GeV (fig.5c) there appears to be an obvious slope difference with the theoretical predictions that none of the individual structure functions can fit. This could be taken as evidence that NLO QCD is inadequate to describe the data in detail, and that new theory such as the inclusion of soft gluon radiation is needed.

IV. CONCLUSIONS

The best state of the art calculation of isolated prompt photon production at NLO was made in this paper. Fragmentation contributions were included fully at NLO and the very latest parametrizations of the proton distributions were used to make comparisons with the CDF data. These comparisons show that there is still some discrepancy between the theoretical predictions and the data which must be addressed before the cross section can be used to extract information on the gluon densities. This discrepancy is now substantially reduced as compared to previous studies, due to a combination of improvements in our

knowledge of the parton densities and inclusion of the fragmentation contributions at NLO.

There is still sufficient spread in the predictions from different parametrizations of the parton densities to indicate that further improvements may be made in this area that would improve the comparison between theory and data. Improvements in the theoretical predictions could also be made by a better understanding of the fragmentation contributions in NLO. In addition, inclusion of soft gluon radiation could also be a possible way of improving the theoretical predictions.

A detailed comparison of two methods of calculating the inclusive and isolated prompt photon cross sections, one using purely analytic techniques and the other using the analytic/Monte Carlo technique was made confirming that the two methods give the same results. In the process a previously unexplained discrepancy between the results of the calculations of refs. [7] and [10] was resolved.

V. ACKNOWLEDGMENTS

I would especially like to thank S. Kuhlmann for running the code of ref. [7], and E. L. Berger and E. Kovacs for helpful discussions. I acknowledge Bob Bailey's help when I was originally learning to implement the Monte Carlo method used in this paper. Special thanks goes to thank Marie Maslowski for friendship and support while carrying out this work. This work was supported by the US Department of Energy, Division of High Energy Physics, Contract number W-31-109-ENG-38.

REFERENCES

- [1] J.F. Owens, Rev. Mod. Phys. **59**, 465 (1987).
- [2] E. L. Berger, X. Guo and J.-W. Qiu, Phys. Rev. Lett. **76**, 2234, (1996); Phys. Rev. **D 54**, 5470, (1996).
- [3] P. Aurenche et. al., ENSLAPP-A-595/96, LPTHEORSAY 96-40, hep-ph/9606287.
- [4] CDF Collaboration, F. Abe *et al.*, Phys. Rev. **D 48**, 2998 (1993); Phys. Rev. Lett. **68**, 2734 (1992).
- [5] P. Aurenche, R. Baier and M. Fontannaz, Phys. Rev. **D42**, 1440 (1990).
- [6] P. Aurenche, R. Baier, A. Douiri, M. Fontannaz, and D. Schiff, Phys. Lett. **140B**, 87 (1984); P. Aurenche, R. Baier, M. Fontannaz, and D. Schiff, Nucl. Phys. **B297**, 661 (1988).
- [7] H. Baer, J. Ohnemus, and J. F. Owens, Phys. Rev. **D42**, 61 (1990); B. Bailey, J. Ohnemus, and J. F. Owens, Phys. Rev. **D46**, 2018 (1992).
- [8] E. L. Berger and J. Qiu, Phys. Lett. **B 248**, 371 (1990); Phys. Rev. **D 44**, 2002 (1991).
- [9] L. E. Gordon and W. Vogelsang Phys. Rev. **D50**, 1901 (1993).
- [10] M. Glück, L. E. Gordon, E. Reya, and W. Vogelsang, Phys. Rev. Lett. **73**, 388 (1994).
- [11] L. E. Gordon and W. Vogelsang Phys. Rev. **D48**, 3136 (1993) and **D49**, 170 (1994).
- [12] F. Aversa, P. Chiappetta, M. Greco and J.Ph. Guillet, Phys. Lett. **B 210**, 225 (1988); 211, 465 (1988); Nucl. Phys. **B327**, 105 (1989).
- [13] M. Glück, E. Reya and A. Vogt, Phys. Rev. **D48**, 116 (1993).
- [14] CDF Collaboration, F. Abe *et al.*, Phys. Rev. Lett. **73**, 2662 (1994).
- [15] J. Huston *et al.*, Phys. Rev. **D 51**, 6139 (1995).

- [16] L. E. Gordon ANL-HEP-PR-96-59.
- [17] H. Baer and M. H. Reno, Phys. Rev. **D 54**, 2017 (1996).
- [18] H. L. Lai *et al.*, CTEQ Collaboration, Phys. Rev. **D51**, 4763 (1995).
- [19] A. D. Martin, R. G. Roberts and W. J. Stirling, DPT/96/44.
- [20] M. Glück, E. Reya and A. Vogt, Z. Phys. **C67**, 433 (1995).
- [21] M. Glück, E. Reya and A. Vogt, Phys. Rev. **D45**, 3986 (1992).
- [22] H. Lai *et al.*, CTEQ Collaboration, MSUHEP-60426, CTEQ-604, hep-ph/9606399.

FIGURE CAPTIONS

[1] (a) Comparison of the inclusive prompt photon cross section plotted vs p_T^γ as predicted by the analytic [9] and analytic/Monte Carlo calculations at $\sqrt{s} = 1.8$ TeV, and $\eta = 0$. (b) Same as (a) but for the isolated cross section with $R = 0.7$ and $\epsilon = 2$ GeV/ p_T^γ . (c) The isolated cross section in (b) broken down into contributions from initial state subprocesses.

[2] (a) Dependence of the isolated cross section on the energy resolution parameter ϵ at fixed $R = 0.7$ for two values of photon p_T as predicted by the analytic and Monte Carlo calculations. (b) Dependence of the isolated cross section on the isolation cone size R for fixed ϵ for the analytic and Monte Carlo calculations.

[3] (a) Ratio of the fragmentation contribution to the isolated cross section to the full isolated cross section, where the fragmentation contribution is calculated using LO and NLO matrix elements. (b) Ratios of the full NLO cross section to the NLO cross section calculated with LO matrix elements for the fragmentation contribution for the isolated and inclusive cases.

[4] (a) Comparison of the full isolated cross section calculated using different parametrizations of parton densities with the CDF data. (b) Same as (a) but for the lower p_T^γ region only. (c) and (d) Plots of the ratio (DATA-THEORY)/THEORY, where THEORY is the full NLO theoretical predictions calculated using the MRSR2 and CTEQ4HJ parametrizations of the proton densities, and DATA are data from the CDF collaboration. The different textured curves are obtained by substituting theoretical predictions made using different parametrizations of the proton densities for the DATA.

[5] (a) Plot of (DATA-THEORY)/THEORY where THEORY is the theoretical predictions obtained using the MRSR4 proton densities in the low p_T^γ region of the CDF data. (b) Same as (a) in the higher p_T^γ region for THEORY given by

the MRSR1 proton densities. (c) as (a) and (b) for the central p_T^γ region for THEORY given by both the MRSR1 and MRSR4 proton densities.

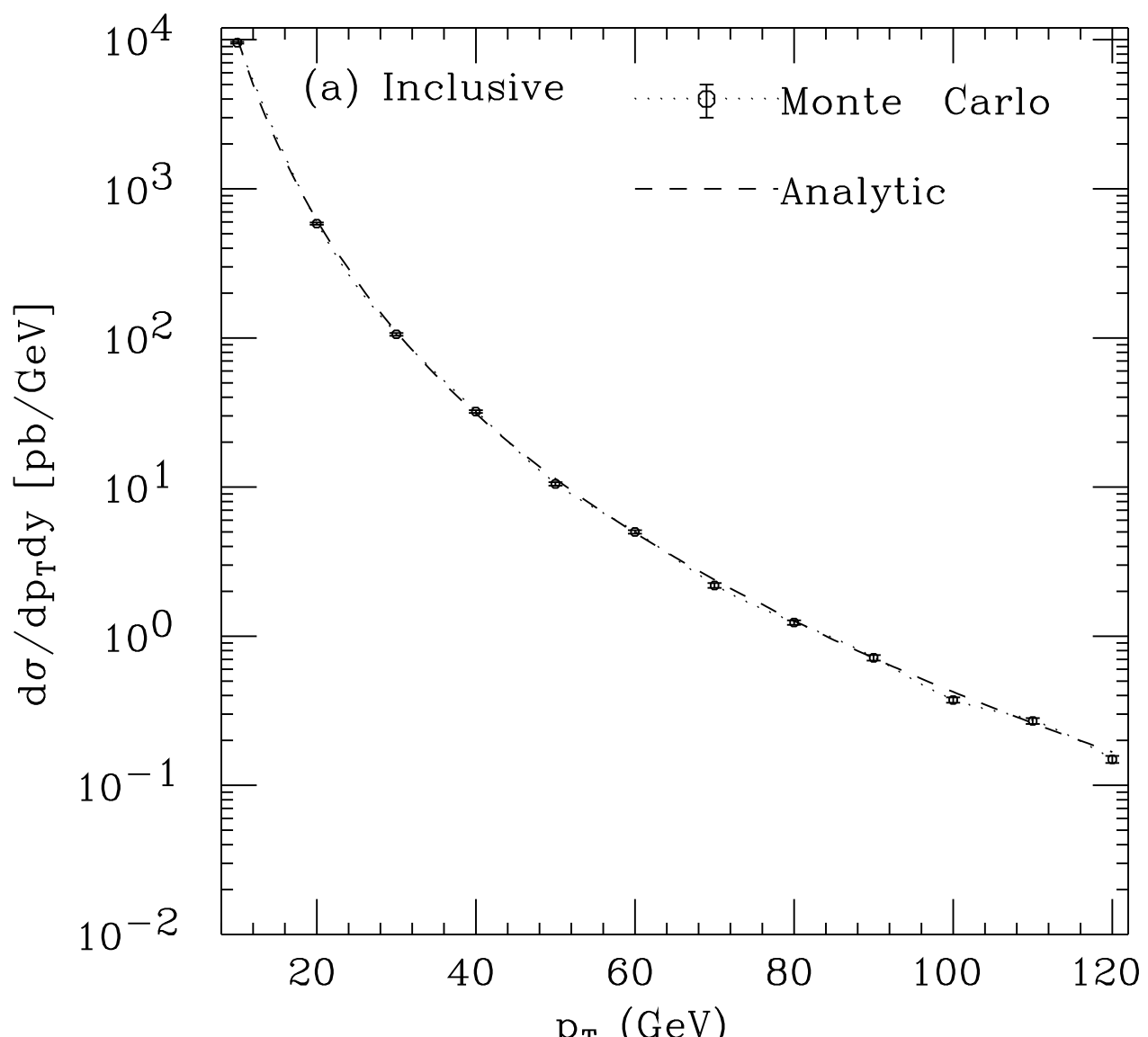


Fig. 1a

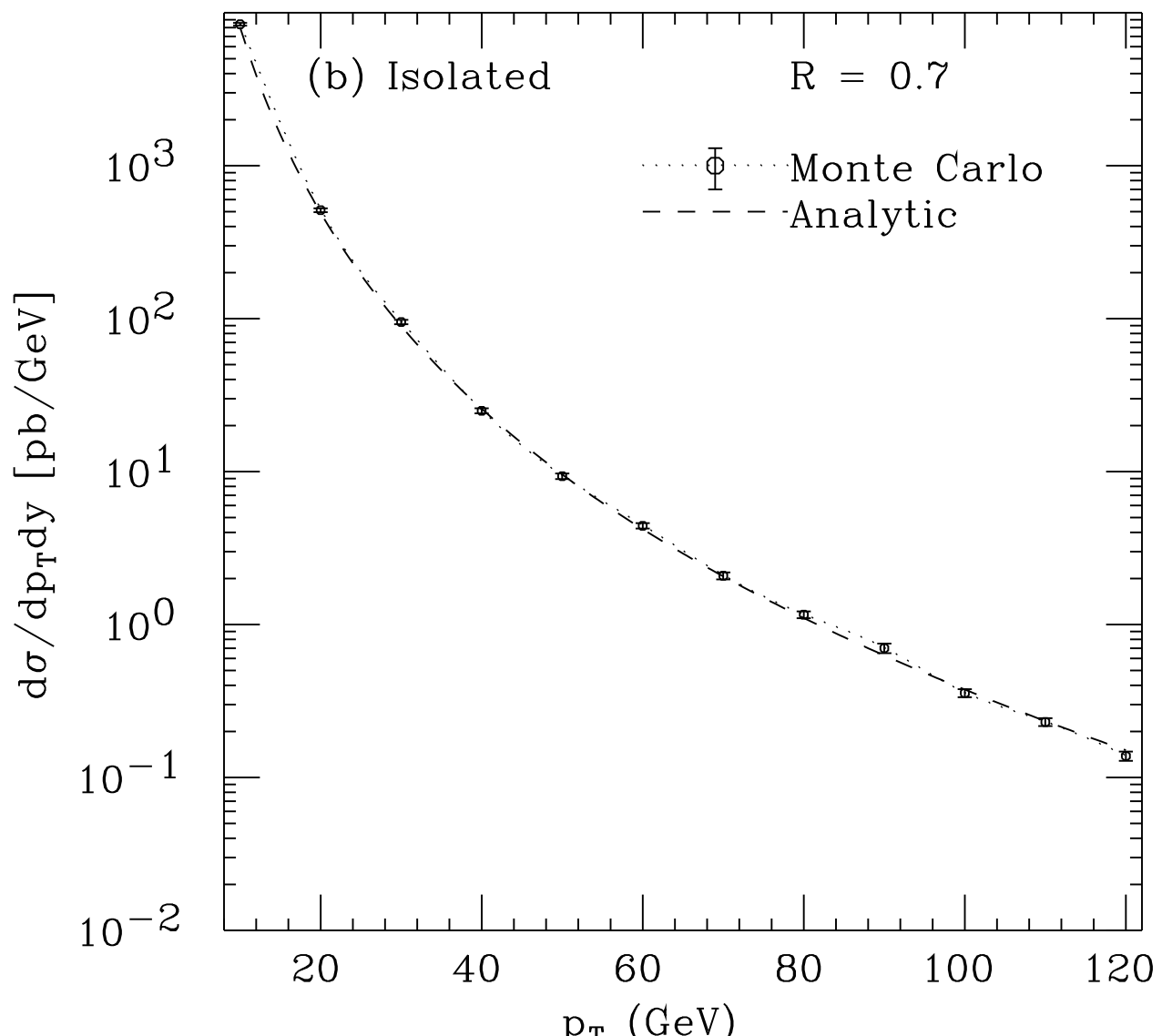


Fig. 1b

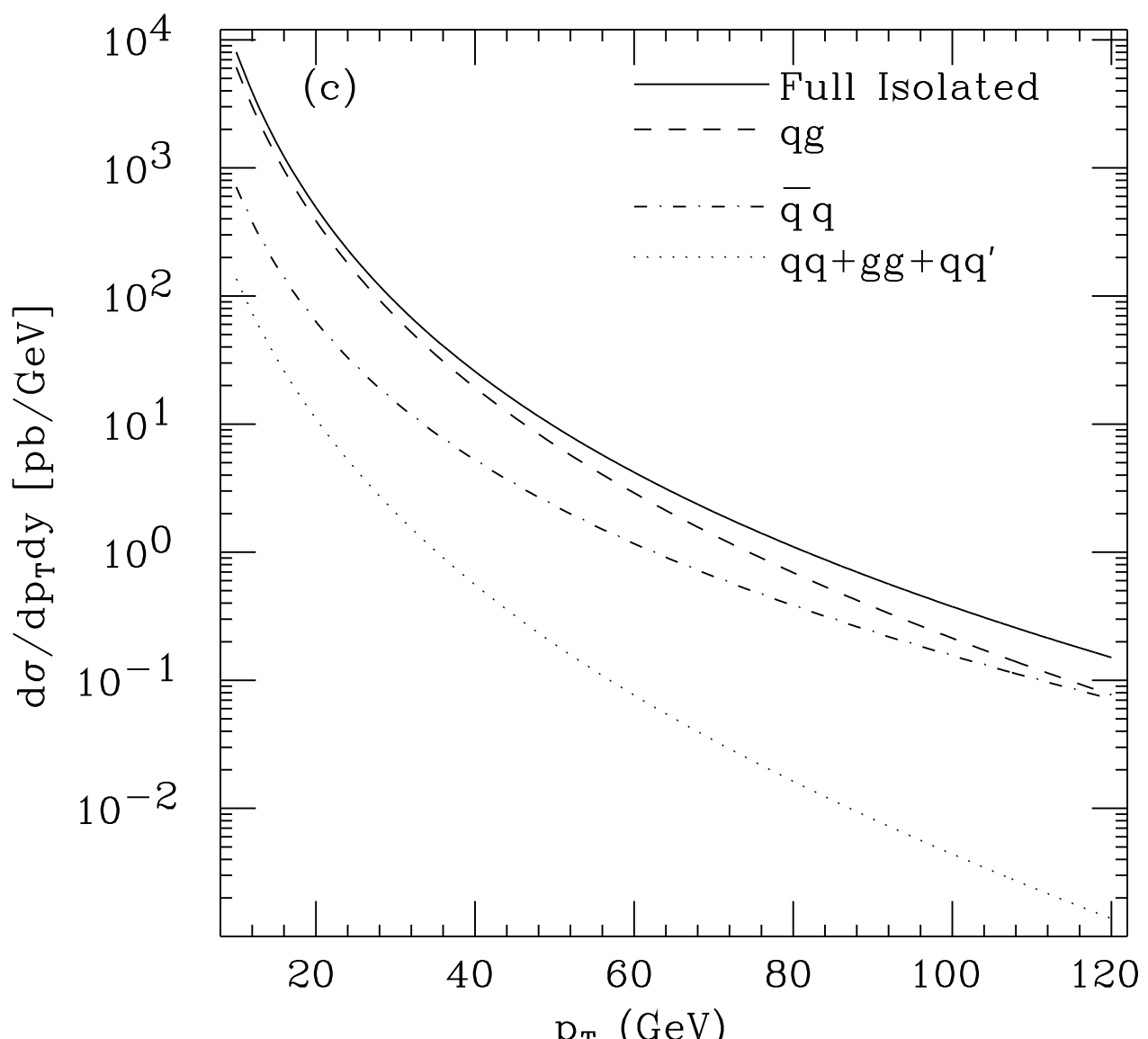


Fig.1c

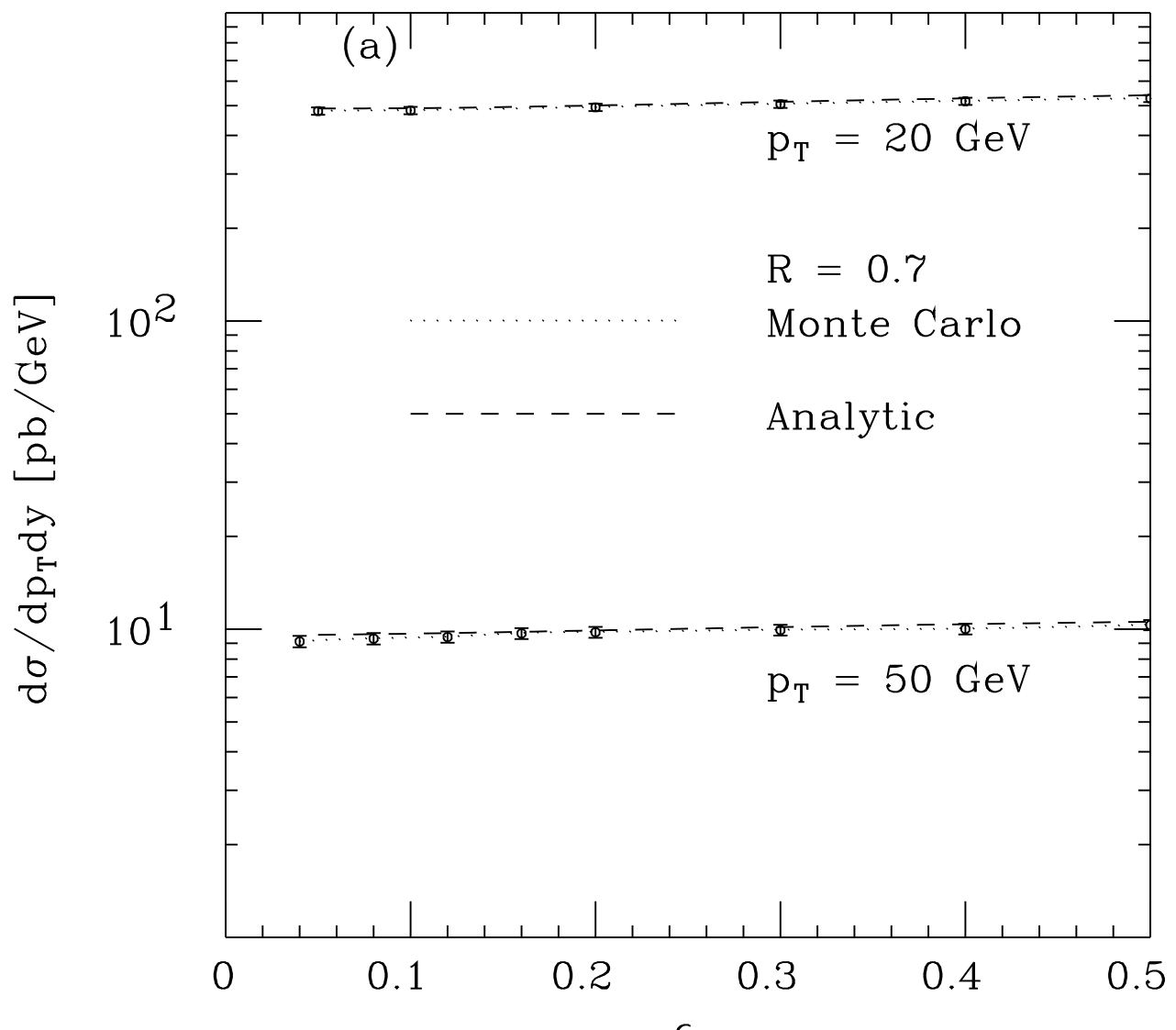


Fig.2a

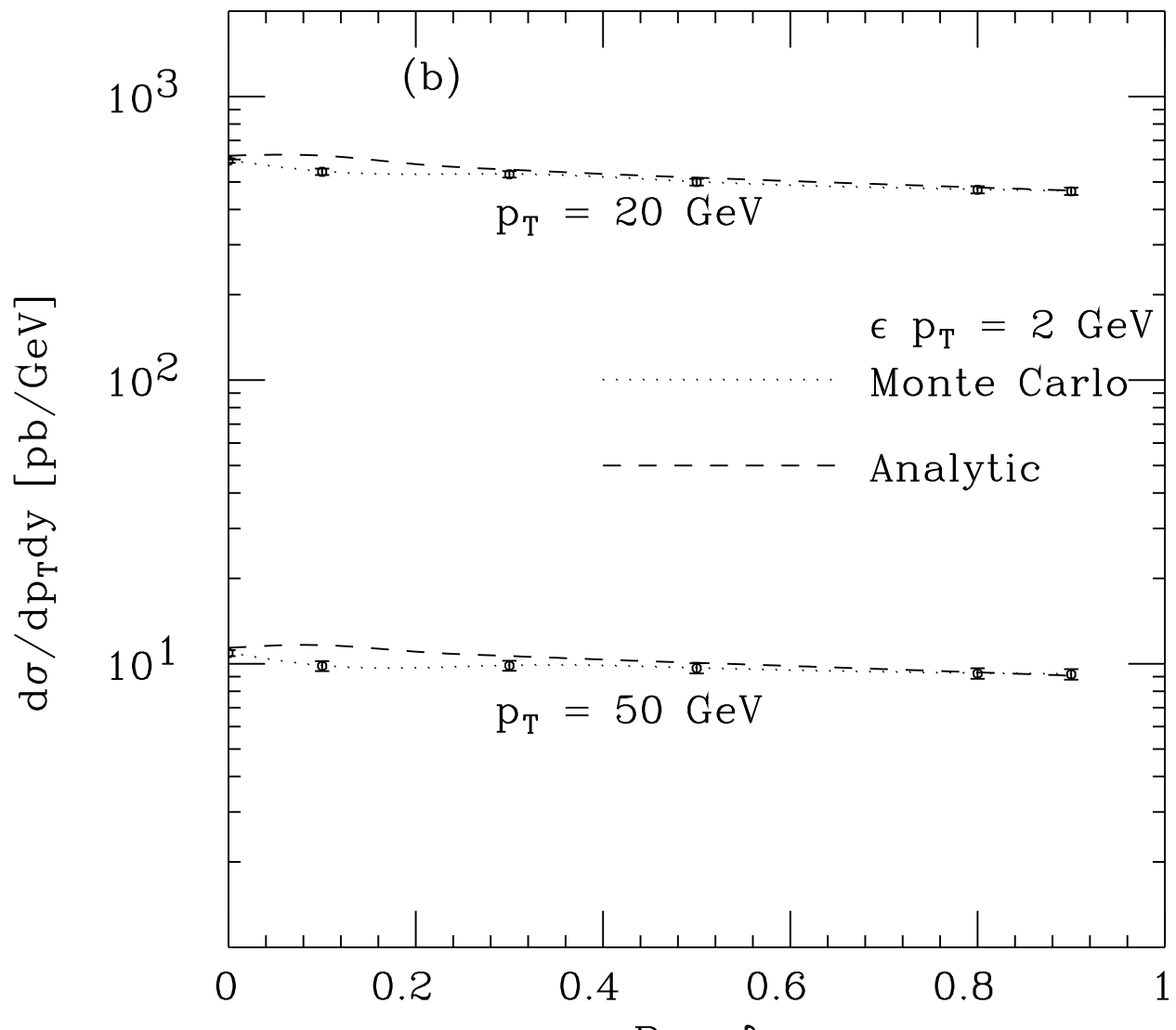


Fig.2b

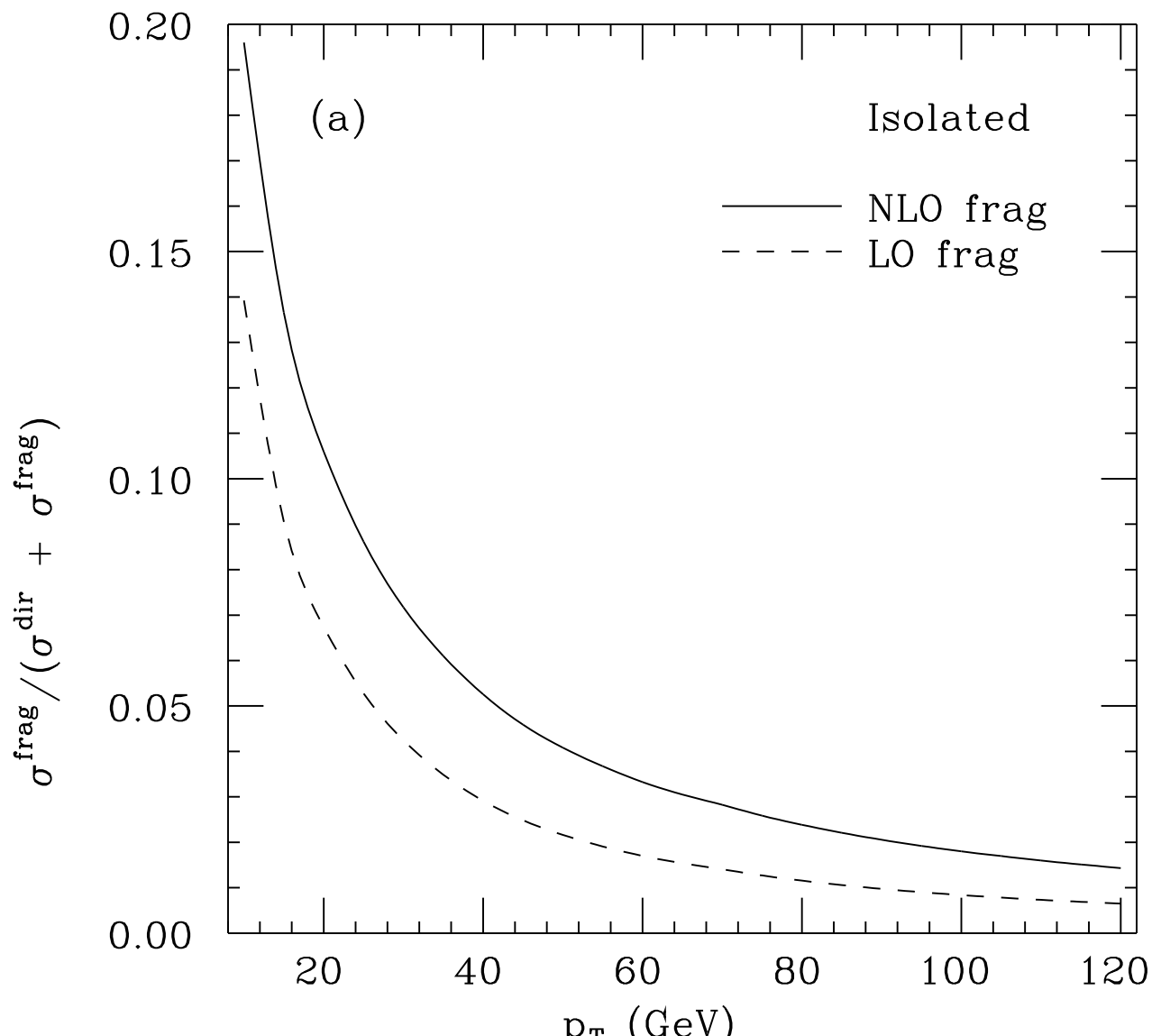


Fig. 3a

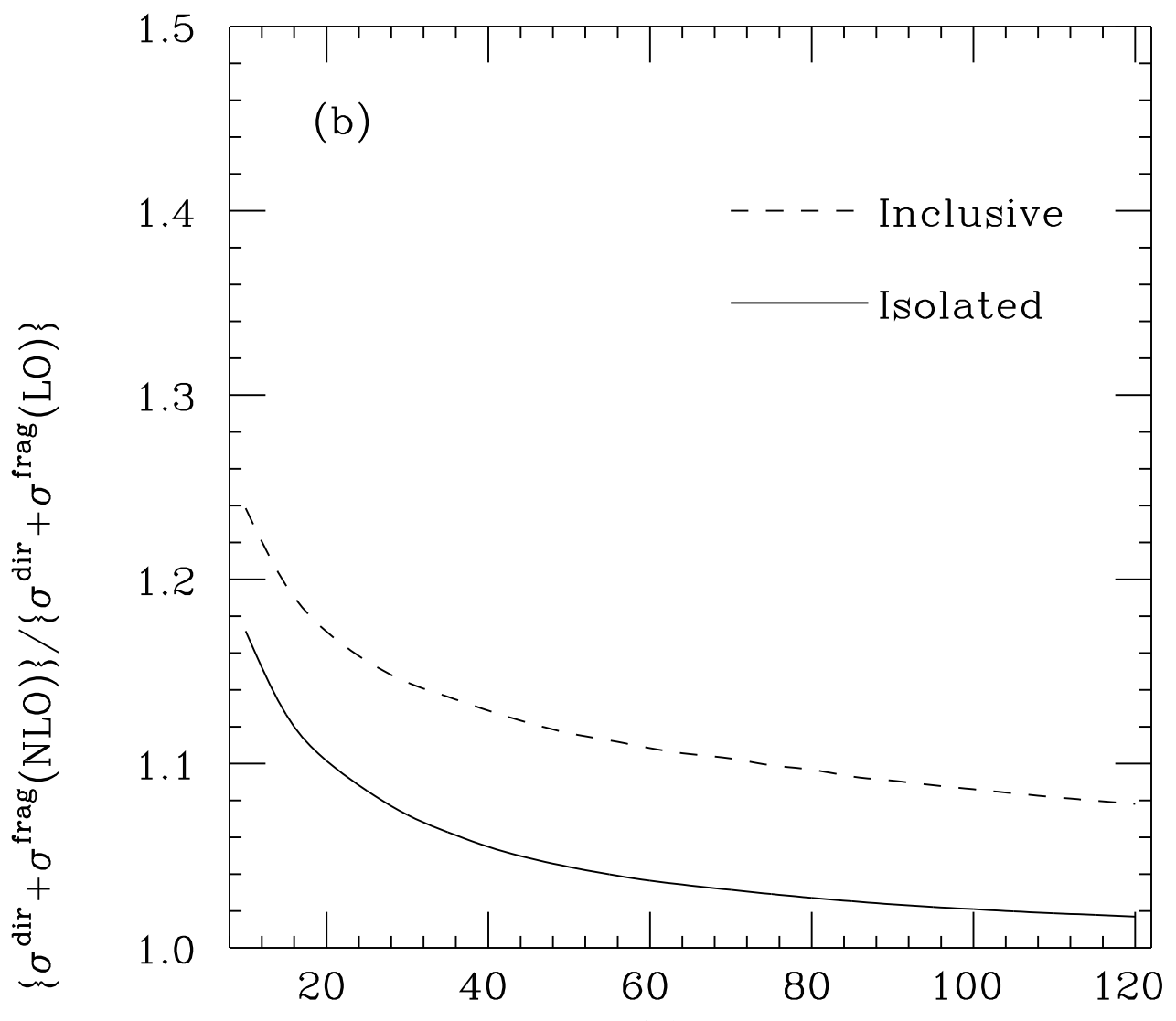


Fig.3b

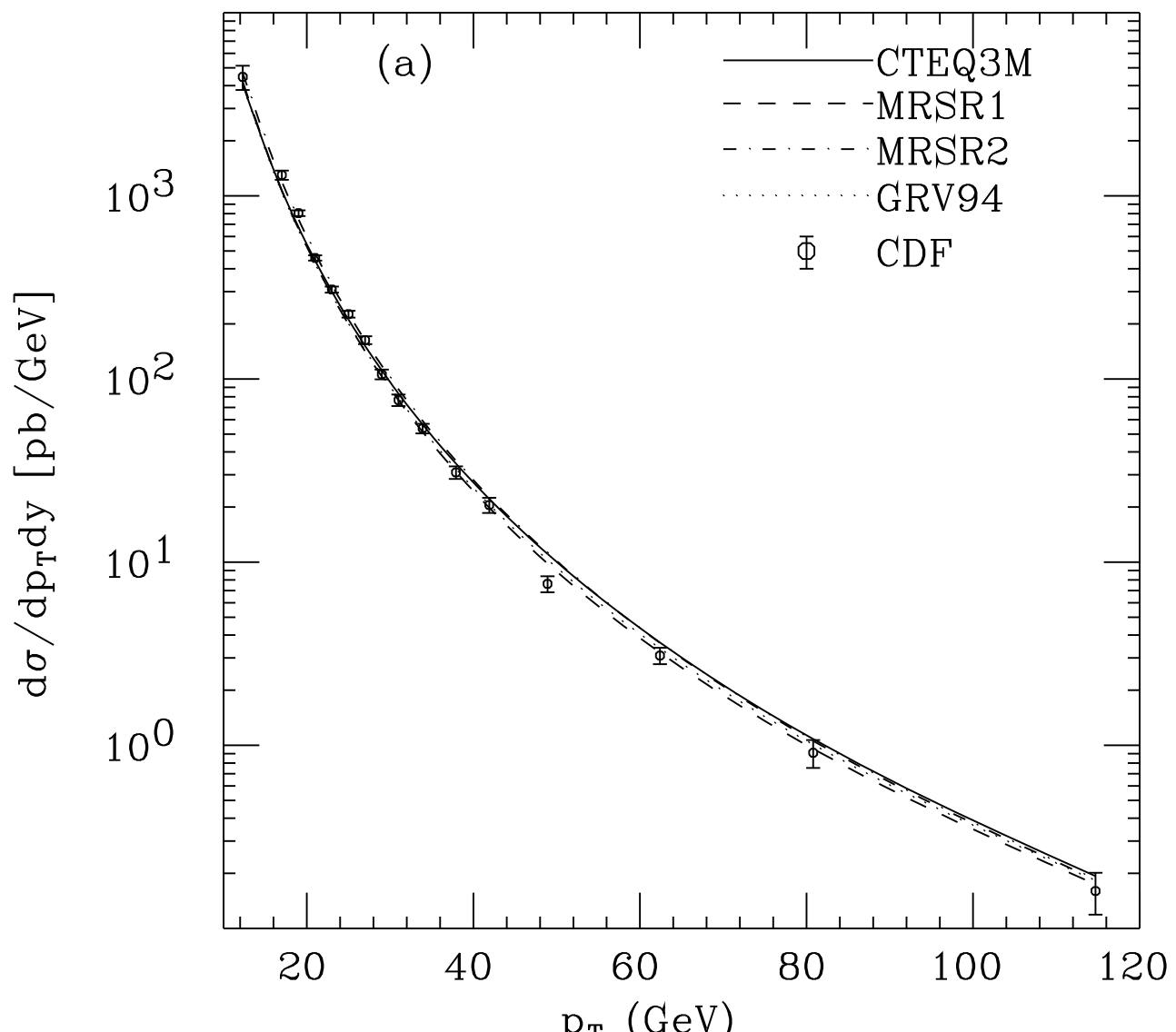


Fig. 4a

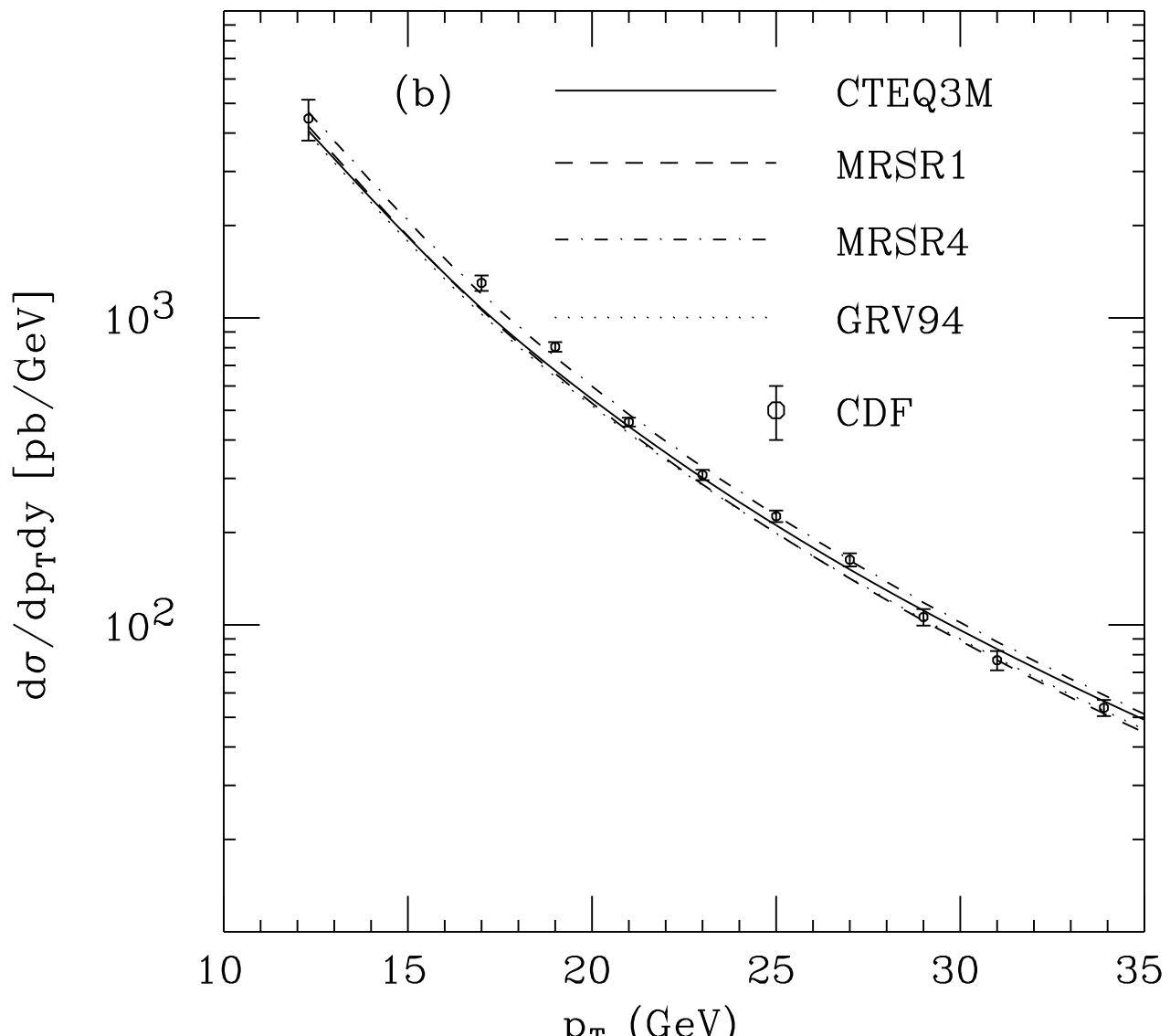


Fig. 4b

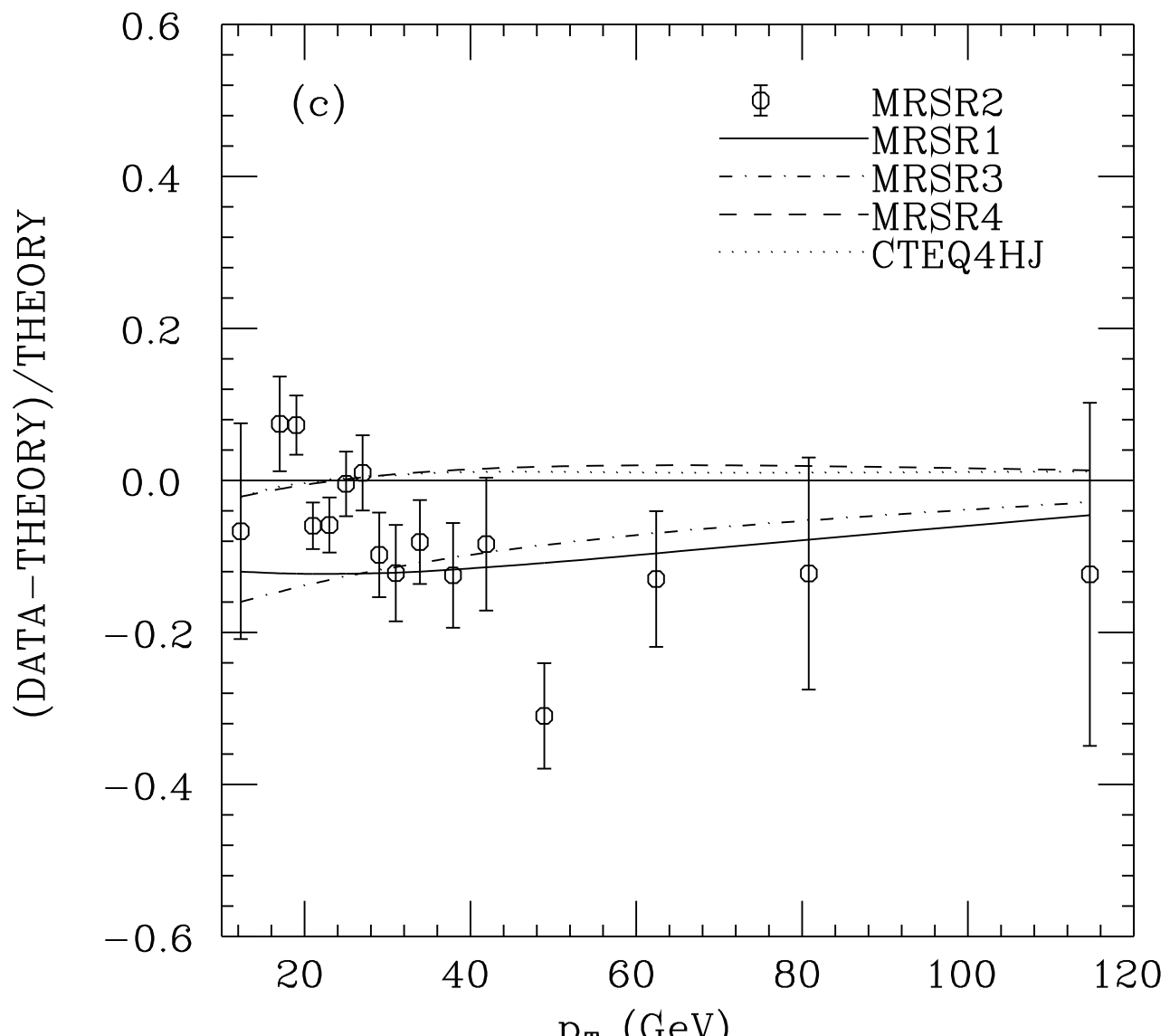


Fig.4c

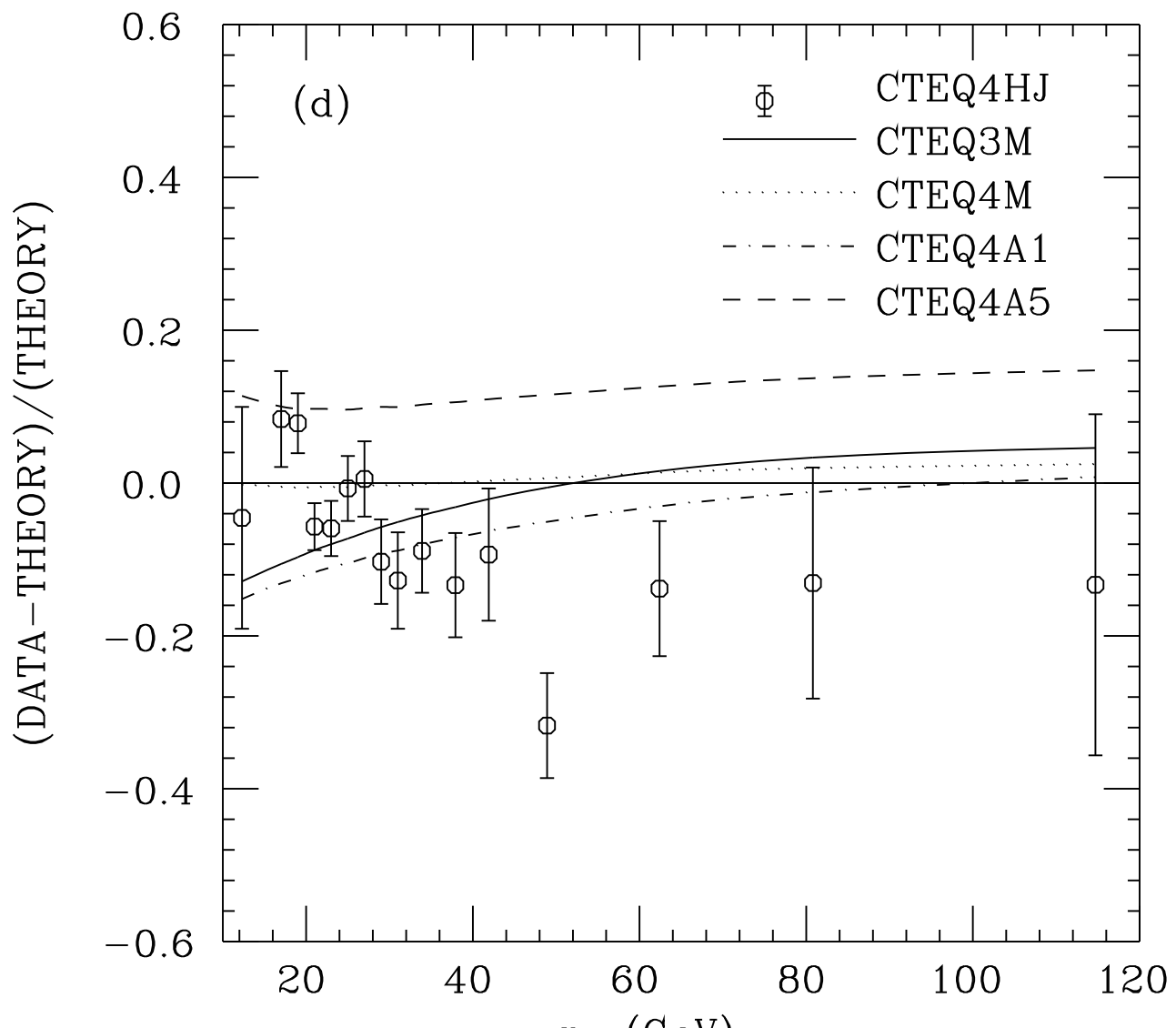
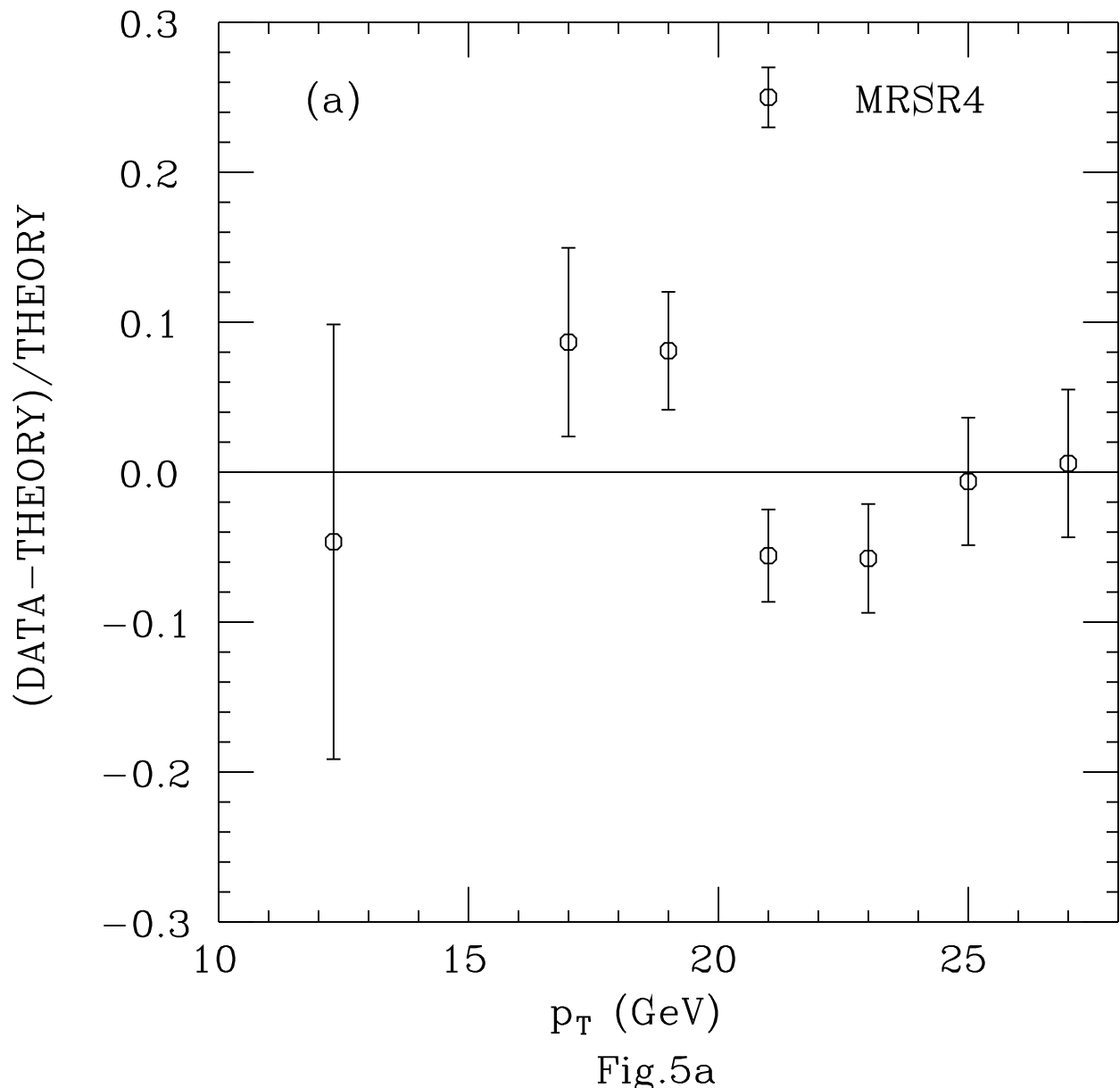


Fig.4d



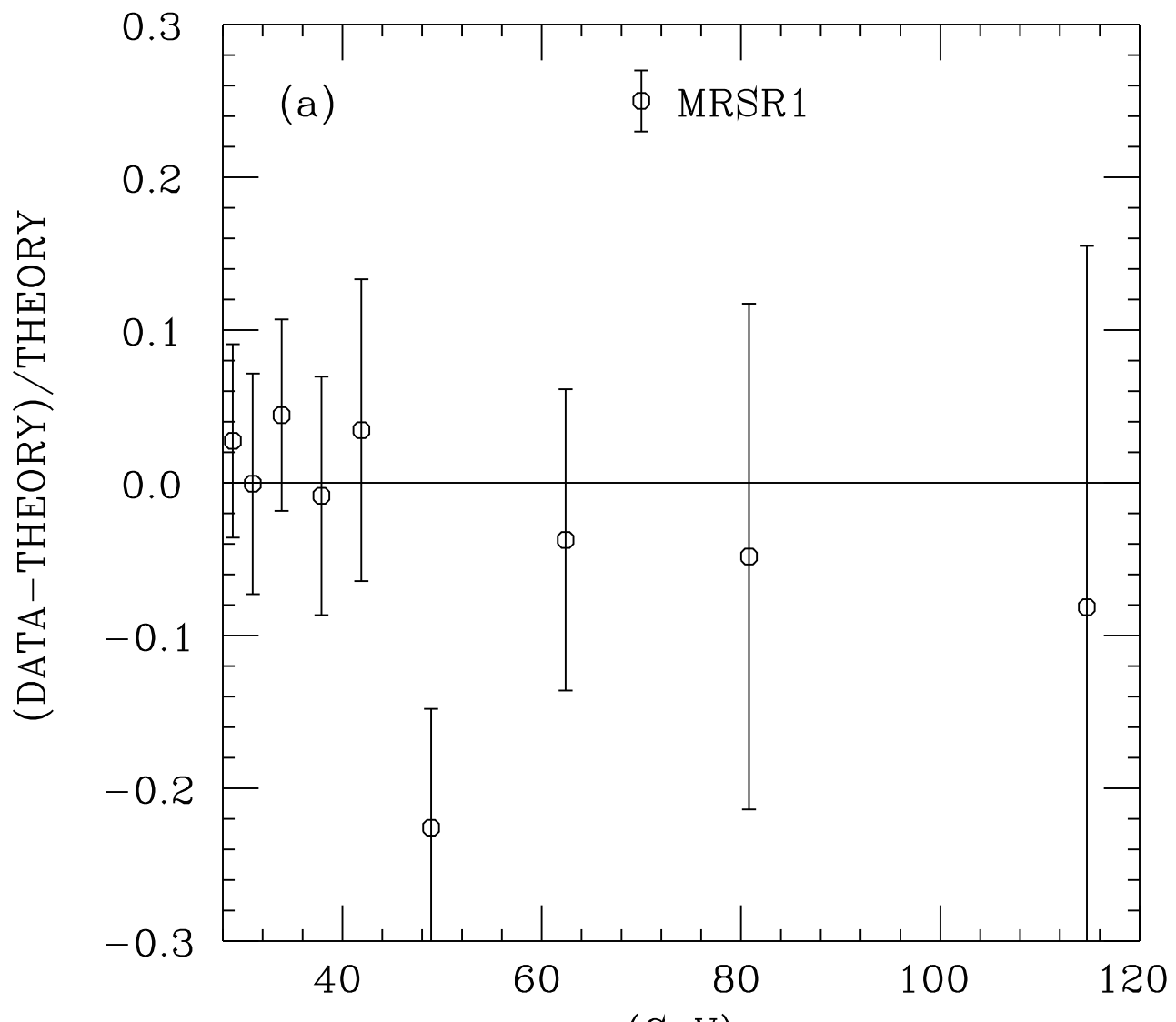


Fig.5b

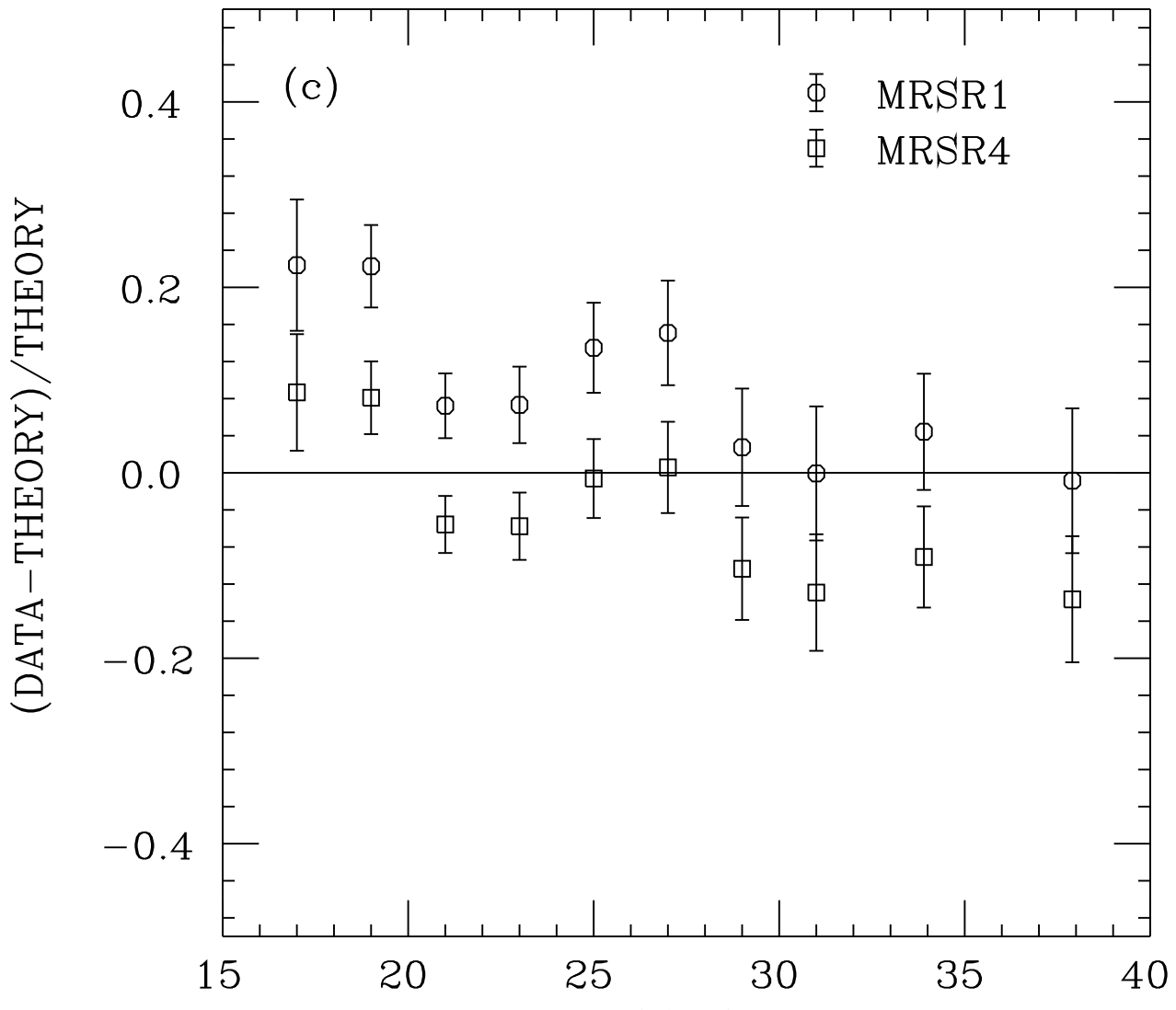


Fig.5c